Static and dynamic coupled perturbed Hartree-Fock vibrational (hyper)polarizabilities of polyacetylene calculated by the finite field nuclear relaxation method

Static and dynamic coupled perturbed Hartree-Fock vibrational (hyper)polarizabilities of polyacetylene calculated by the finite field nuclear relaxation method

Valentina Lacivita, Michel Rérat, Bernard Kirtman, Roberto Orlando, Matteo Ferrabone et al.

Citation: J. Chem. Phys. **137**, 014103 (2012); doi: 10.1063/1.4731266
View online: http://dx.doi.org/10.1063/1.4731266
View Table of Contents: http://jcp.aip.org/resource/1/JCPSA6/v137/i1
Published by the American Institute of Physics.

Static and dynamic coupled perturbed Hartree-Fock vibrational (hyper)polarizabilities of polyacetylene calculated by the finite field nuclear relaxation method

Valentina Lacivita,[1] Michel Rérat,[2] Bernard Kirtman,[3] Roberto Orlando,[1] Matteo Ferrabone,[1] and Roberto Dovesi[1]
[1]*Dipartimento di Chimica, Università di Torino, and NIS–Nanostructured Interfaces and Surfaces–Centre of Excellence, Via P. Giuria 7, 10125 Torino, Italy*
[2]*Equipe de Chimie Physique, IPREM UMR5254, Universite de Pau et des Pays de l'Adour 64000 Pau, France*
[3]*Department of Chemistry and Biochemistry, University of California, Santa Barbara, California 93106, USA*

(Received 25 January 2012; accepted 8 June 2012; published online 3 July 2012)

The vibrational contribution to static and dynamic (hyper)polarizability tensors of polyacetylene are theoretically investigated. Calculations were carried out by the finite field nuclear relaxation (FF-NR) method for periodic systems, newly implemented in the CRYSTAL code, using the coupled perturbed Hartree-Fock scheme for the required electronic properties. The effect of the basis set is also explored, being particularly important for the non-periodic direction perpendicular to the polymer plane. Components requiring a finite (static) field in the longitudinal direction for evaluation by the FF-NR method were not evaluated. The extension to that case is currently being pursued. Whereas the effect on polarizabilities is relatively small, in most cases the vibrational hyperpolarizability tensor component is comparable to, or larger than the corresponding static electronic contribution.
 [http://dx.doi.org/10.1063/1.4731266]

I. INTRODUCTION

Even before the advent of quantum mechanics there has been much interest in the various properties exhibited by molecules and materials in response to external electric fields. For spatially uniform perturbing fields this response is governed by the electric dipole moment or polarization vector. The dipole moment, in turn, contains a permanent component plus induced components arising from the linear polarizability and the nonlinear hyperpolarizabilities. Each of these properties includes contributions from both the electronic and nuclear motions. In this paper, we will focus on the role of nuclear motions as they affect both the static and dynamic (hyper)polarizabilities.

A major advance in the field occurred about 20 years ago, with publication of Bishop and Kirtman's general perturbation treatment (BKPT) (Ref. 1) based on a double (mechanical and electrical) harmonic initial approximation. They developed closed form expressions for the ω-dependent (ω is the frequency of the electric field) pure vibrational (hyper)polarizabilities, which are due to vibrational transitions on the Born-Oppenheimer ground electronic state potential energy surface (much smaller zero-point vibrational averaging contributions are treated separately).

Although there continue to be many applications of BKPT, the computations can be extensive since they require determination of harmonic and anharmonic vibrational force constants as well as first and higher order (anharmonic) electrical property derivatives. Even in the double harmonic approximation the calculation of quadratic vibrational force constants can be computationally demanding. In order to streamline the computational effort a closely related, but non-perturbative, finite field nuclear relaxation (FF-NR) method was proposed about five years later by Bishop, Hasan, and Kirtman.[2] The key step in the FF-NR method is a geometry optimization carried out in the presence of a finite static field. This optimization implicitly contains the information about harmonic and anharmonic vibrational parameters needed to obtain vibrational (hyper)polarizabilities. Thus, no force constants or electric property derivatives need to be explicitly calculated. The vibrational (hyper)polarizabilities thus determined take into account all double harmonic contributions plus all first-order anharmonic terms and, in one case, a second-order anharmonic contribution. A simple extension of the original procedure leads to a treatment that, in principle, can account for all remaining contributions not evaluated in the original FF-NR method.[3]

Both static and dynamic properties are determined by the FF-NR method. The latter are obtained within the so-called infinite optical frequency approximation (IOFA), which corresponds to ignoring terms involving (ν^2/ω^2) compared to unity where ν is a vibrational frequency. At typical laser-optical frequencies, the IOFA is found to be well-satisfied. Among all the linear and nonlinear optical processes for which the infinite frequency limit is applicable, the only one not contained in the original formulation is the intensity-dependent refractive index, i.e., $\gamma^{nr}(-\omega; \omega, -\omega, \omega)$, also known as degenerate four-wave mixing. Recently, a modification has been presented that fills in this lacuna.[4]

It should be noted that the FF-NR method, as well as BKPT, applies specifically to the non-resonant regime. That is to say, it is assumed that the laser-optical frequency may be neglected in comparison with electronic transition frequencies. A response formalism that can be used to calculate the terms that are thereby omitted has recently been presented.[5]

However, in the IOFA and in the static limit (the cases studied here) these additional contributions have been shown to vanish.[6]

The FF-NR method has been widely applied to molecules. The first application to an infinite periodic nanomaterial, namely, an $(n, 0)$ zigzag BN nanotube, was published very recently.[7] Preliminary coupled perturbed Kohn-Sham calculations were performed, in that case, for transverse (hyper)polarizabilities of small diameter tubes at the B3LYP level, using the CRYSTAL code.[8,9] Even more recently, these results were extended to larger nanotubes – up to $(36, 0)$ – and to the non-diagonal or mixed tensor components.

In the present work, we apply the FF-NR method to another typical 1D periodic system, i.e., polyacetylene (PA), which has served as the prototype for the effect of π-electron conjugation on (linear and) nonlinear optical properties since the 80's.[10,11] π-conjugated quasi-linear polymers have been of great interest for technological applications as they show very large and ultrafast nonlinear optical (NLO) responses. In addition, they are easy to modify chemically in order to meet specific design requirements. In the case of PA, we focus on several of the most common third-order properties (second-order properties are annihilated by centrosymmetry) including the static second hyperpolarizability $\gamma(0; 0, 0, 0)$, electric field induced second harmonic generation $\gamma(-2\omega; \omega, \omega, 0)$ and the DC Kerr effect $\gamma(-\omega; \omega, 0, 0)$. Here, ω is the non-resonant optical frequency of an external electric field.

Our major emphasis is on establishing the relative magnitude of vibrational versus electronic contributions. In doing so, we confirm and extend the methodology previously employed for BN nanotubes. Moreover, the results allow us to generalize some of the conclusions found earlier.

The FF-NR method involves calculating the structural distortion due to a finite field followed by evaluation of the electronic dipole moment μ, polarizability α, and first hyperpolarizability β tensors at the relaxed geometry. Then, by comparison with static electronic (hyper)polarizabilities at the equilibrium geometry, the vibrational hyperpolarizability tensors are obtained. As in the previous paper on BN nanotubes, although many tensor components are determined, there are some exceptions due to the fact that the special treatment for a finite field in the periodic direction has not yet been implemented in the CRYSTAL code.[12] Contributions from so-called collective modes, which are known to be small for PA[13,14] (i.e., compared to the corresponding electronic property), are also omitted. In addition to the geometry relaxation, the effect of the applied field on the band-gap and minimum energy is determined.

Our calculations were carried out at the Hartree-Fock (HF) level of theory since previous literature has shown that conventional density functionals form the Density Functional Theory (DFT) do not perform nearly as well for the electronic polarizability and hyperpolarizability of PA (in comparison with correlated MP2 results; see, for example, Refs. 15 and 16). By introducing an effective counteracting field, the exact exchange included in HF tends to compensate for the large overpolarization obtained with conventional DFT functionals;[15,17–22] electron correlation, it turns out, plays a much smaller role.

In Secs. II and III we review the FF-NR methodology and provide computational details for treatment of π-conjugated systems by means of the CRYSTAL program. Our results are presented and analyzed in Sec. IV. Finally, Sec. V contains a summary of key aspects and a brief discussion of possible further applications/development of the FF-NR method for periodic systems.

II. METHOD

A. The vibrational contribution to polarizability

The electronic (hyper)polarizabilities (with zero-point averaging included) do not take into account so-called *pure* vibrational effects, which can be quite important. Diagonal components of the static polarizability, for example, may be approximated as the sum of two terms,

$$\alpha^0 = \alpha^e + \sum_j \frac{\overline{Z}_j^2}{\nu_j^2}, \tag{1}$$

where α^e is the electronic contribution, frequently indicated by α^∞. The (pure) vibrational (sometimes known as *ionic*) contribution is given, in the double harmonic approximation, by the second term on the right hand side. In that term, $\overline{Z}_j$ is a mass-weighted effective mode Born charge (also known as the dipole moment derivative in molecular theory) and ν_j is a harmonic vibrational frequency. For periodic systems Born charges may be estimated, as in the CRYSTAL code, either through the Berry phase approach[23,24] or by using Wannier functions, i.e., localized crystal orbitals.[25]

The (double harmonic) vibrational contribution may, alternatively, be computed by the FF-NR method without explicitly evaluating either $\overline{Z}_j$ or ν_j. As previously shown formally, and numerically verified for molecular systems,[2] the FF-NR result is identical (within numerical accuracy) to that obtained from Eq. (1). This has been confirmed for periodic systems (see Ref. 26) and for the computational schemes implemented in the CRYSTAL code (at this time for non-periodic directions only) in connection with application to periodic BN nanotubes (see Ref. 12). In the following, we will show the equivalence for PA as well.

B. The FF-NR scheme

In the current paper, we evaluate components not only of the static (double harmonic) vibrational linear polarizability, α^0, but also of static and dynamic (nuclear relaxation) vibrational hyperpolarizabilities by means of the FF-NR method.[2] If we denote the equilibrium geometry in a static electric field (F) by R_F, and without the field by R_0, then a Taylor series expansion for a field-dependent dipole moment component at the two geometries yields,

$$\mu_t(R_0, F) = \mu_t(R_0, 0) + \sum_u \alpha^e_{tu} F_u + \frac{1}{2} \sum_{u,v} \beta^e_{tuv} F_u F_v + \frac{1}{6} \sum_{u,v,w} \gamma^e_{tuvw} F_u F_v F_w + \cdots \tag{2}$$

and

$$\mu_t(R_F, F) = \mu_t(R_0, 0) + \sum_u a^{\mu}_{tu} F_u + \frac{1}{2}\sum_{u,v} b^{\mu}_{tuv} F_u F_v + \frac{1}{6}\sum_{u,v,w} g^{\mu}_{tuvw} F_u F_v F_w + \cdots . \quad (3)$$

In Eq. (2) the superscript e refers to the static pure electronic value. Experimentally it may be obtained by carrying out non-resonant measurements at sufficiently high frequency so that vibrations cannot contribute and, then extrapolating to the zero frequency limit. On the other hand, static field measurements yield directly the coefficients on the right hand side of Eq. (3), which include vibrational contributions at the field-free equilibrium geometry. In using Eqs. (2) and (3) it is implicitly assumed that zero-point vibrational averaging effects may be neglected. Thus, the dipole moment at the field-dependent equilibrium geometry yields the coefficients (see again Ref. 2),

$$a^{\mu}_{tu} = \alpha^{e}_{tu} + \alpha^{nr}_{tu}(0; 0), \quad (4)$$

$$b^{\mu}_{tuv} = \beta^{e}_{tuv} + \beta^{nr}_{tuv}(0; 0, 0), \quad (5)$$

$$g^{\mu}_{tuvw} = \gamma^{e}_{tuvw} + \gamma^{nr}_{tuvw}(0; 0, 0, 0), \quad (6)$$

where the superscript nr indicates the nuclear relaxation approximation for the (field-free) equilibrium vibrational contribution and the (circular) frequencies of the applied fields are given (as usual) in parentheses, e.g., $\beta(0; 0, 0) = \beta(-\omega_\sigma; \omega_1, \omega_2)$ with static applied fields $\omega_i = 0$ and $\omega_\sigma = \omega_1 + \omega_2$. Note that the right hand side of Eq. (4) is, in principle, identical to the total static polarizability given by Eq. (1), since in either case only harmonic vibrational terms are included. However, the static hyperpolarizabilities also contain contributions due to anharmonic force constants and anharmonic electrical property derivatives (see, for example, Ref. 27). In order to isolate the nuclear relaxation term one can either subtract the analytically determined electronic term or calculate the difference between numerical values from Eqs. (2) and (3). Similar expansions may be carried out for α^e,

$$\alpha^{e}_{tu}(R_0, F) = \alpha^{e}_{tu}(R_0, 0) + \sum_v \beta^{e}_{tuv} F_v + \frac{1}{2}\sum_{v,w} \gamma^{e}_{tuvw} F_v F_w + \cdots \quad (7)$$

$$\alpha^{e}_{tu}(R_F, F) = \alpha^{e}_{tu}(R_0, 0) + \sum_v b^{\alpha}_{tuv} F_v + \frac{1}{2}\sum_{v,w} g^{\alpha}_{tuvw} F_v F_w + \cdots \quad (8)$$

as well as β^e,

$$\beta^{e}_{tuv}(R_0, F) = \beta^{e}_{tuv}(R_0, 0) + \sum_w \gamma^{e}_{tuvw} F_w + \cdots \quad (9)$$

$$\beta^{e}_{tuv}(R_F, F) = \beta^{e}_{tuv}(R_0, 0) + \sum_w g^{\beta}_{tuvw} F_w + \cdots , \quad (10)$$

where

$$b^{\alpha}_{tuv} = \beta^{e}_{tuv} + \beta^{nr}_{tuv}(-\omega; \omega, 0)|_{\omega\to\infty}, \quad (11)$$

$$g^{\alpha}_{tuvw} = \gamma^{e}_{tuvw} + \gamma^{nr}_{tuvw}(-\omega; \omega, 0, 0)|_{\omega\to\infty}, \quad (12)$$

$$g^{\beta}_{tuvw} = \gamma^{e}_{tuvw} + \gamma^{nr}_{tuvw}(-2\omega; \omega, \omega, 0)|_{\omega\to\infty}. \quad (13)$$

In those instances where the geometry is not specified it is R_0, and omitted frequencies are zero. The subscript $\omega \to \infty$ in Eqs. (11)–(13) refers to the IOFA (see Sec. I). In addition to harmonic terms, first-order anharmonic contributions are also included for $\gamma^{nr}(-\omega; \omega, 0, 0)|_{\omega\to\infty}$ (see Ref. 2); for the other two nonlinear optical processes, $\beta^{nr}(-\omega; \omega, 0)|_{\omega\to\infty}$ and $\gamma^{nr}(-2\omega; \omega, \omega, 0)|_{\omega\to\infty}$, the first-order anharmonicity terms vanish.

The measured values of NLO properties ordinarily correspond to the sum of vibrational and electronic contributions. In principle, the two may be separated experimentally as well as computationally. For the former this requires frequency-dependent measurements, as discussed above for α and implied in passing for hyperpolarizabilities by Shelton.[28]

C. Geometry, symmetry, and non-zero components of the tensors

A finite field is applied along the non-periodic directions (y, z, and mixed $y = z$) to obtain the various non-zero tensor components of the vibrational (hyper)polarizabilities discussed below. We consider here an all-trans polyacetylene lying in the xy plane, with alternating double and single C−C bonds along the x periodic direction (a double C−C bond is included within each unit cell). The center of the unit cell is an inversion center (which annihilates odd order energy perturbation terms, i.e., μ and β in our case) and lies on a C_2 axis perpendicular to the σ_h^{xy} mirror plane. The σ_h^{xy} mirror plane relates directions z and $-z$, so that all the components of the α and γ tensors containing an odd number of z indices vanish.

γ is a fourth-order tensor consisting of $3^4 = 81$ components, γ_{tuvw}. Several tensor components are null or equivalent either by point group symmetry or permutation of indices, the latter depending on the number of static field indices. For example, in the case of $\gamma^{nr}_{tuVW}(-\omega; \omega, 0, 0)|_{\omega\to\infty}$ only the permutations $\mathcal{P}_{t,u}$ (associated with the $\omega \to \infty$ limit) and $\mathcal{P}_{V,W}$ (between two static fields) leave the property invariant.

Given the number ($m = 4$, 2, or 1) of static fields, the nuclear relaxation contributions to the second hyperpolarizability can be distinguished into (a) $\gamma^{nr}_{4,tuvw} = \gamma^{nr}_{TUVW}(0; 0, 0, 0)$, (b) $\gamma^{nr}_{2,tuvw} = \gamma^{nr}_{tuVW}(-\omega; \omega, 0, 0)|_{\omega\to\infty}$, and (c) $\gamma^{nr}_{1,tuvw} = \gamma^{nr}_{tuvW}(-2\omega; \omega, \omega, 0)|_{\omega\to\infty}$. Table I reports the independent components for the three cases above. The components $\gamma^{nr}_{m,tuvw}$ are divided, in turn, into four subsets, namely, (i) *tttt*, (ii) *tttu*, (iii) *ttuu*, and (iv) *tuvv*. Parentheses indicate components which are null by symmetry ($z \leftrightarrow -z$). Highlighted components are those calculated in the present work since

TABLE I. Independent components of PA nuclear relaxation second hyperpolarizability tensor, γ_n^{nr}. There are four classes (first column), depending upon the number of repeated indices and three subgroups within each class. The latter depend upon whether the static field(s) in the nonlinear process are associated with 4 (column (a)), 2 (column (b)), or 1 (column(c)) directional indices (in capital letters). Components that vanish due to planar symmetry are included in parentheses. Of the remainder only the highlighted ones were calculated as they do not require application of a finite field along the periodic direction in the FF-NR method. The row labelled $\mathcal{M}$ specifies the multiplicity. There are N_{ind} independent components, of which $N_{\neq 0}$ do not vanish due to symmetry, and N_{calc} were computed in the present work.

		(a)	(b)			(c)		
Class	$\mathcal{M}$	1	1	2	4	1	3	6
(i)		*XXXX*	*xxXX*	…	…	*xxxX*	…	…
		YYYY	**yyYY**	…	…	**yyyY**	…	…
		ZZZZ	**zzZZ**	…	…	**zzzZ**	…	…
	$\mathcal{M}$	4	1	2	4	1	3	6
(ii)		*XXXY*	-	*xxXY*	…	**xxxY**	*xxyX*	…
		(*XXXZ*)	…	(*xxXZ*)	…	(*xxxZ*)	(*xxzX*)	…
		YYYX	…	*yyYX*	…	*yyyX*	**xyyY**	…
		(*YYYZ*)	…	(*yyYZ*)	…	(*yyyZ*)	(*zyyY*)	…
		(*ZZZX*)	…	(*zzZX*)	…	(*zzzX*)	(*xzzZ*)	…
		(*ZZZY*)	…	(*zzZY*)	…	(*zzzY*)	(*yzzZ*)	…
		…	…	*xyXX*	…	…	…	…
		…	…	(*xzXX*)	…	…	…	…
		…	…	**xyYY**	…	…	…	…
		…	…	(*zyYY*)	…	…	…	…
		…	…	(*xzZZ*)	…	…	…	…
		…	…	(*yzZZ*)	…	…	…	…
	$\mathcal{M}$	6	1	2	4	1	3	6
(iii)		*XXYY*	**xxYY**	…	*xyXY*	…	**xxyY**	…
		XXZZ	**xxZZ**	…	*xzXZ*	…	**xxzZ**	…
		YYZZ	**yyZZ**	…	**yzYZ**	…	**yyzZ**	…
		…	**zzYY**	…	…	…	**yzzY**	…
		…	*yyXX*	…	…	…	*xyyX*	…
		…	*zzXX*	…	…	…	*xzzX*	…
	$\mathcal{M}$	12	1	2	4	1	3	6
(iv)		(*XXYZ*)	…	(*xxYZ*)	(*xyXZ*)	…	(*xxyZ*)	(*xyzX*)
		(*YYXZ*)	…	(*yyXZ*)	(*yzXY*)	…	(*yyxZ*)	(*xyzY*)
		ZZXY	…	*zzXY*	*yzXZ*	…	*zzyX*	**xyzZ**
		…	…	(*yzXX*)	(*xzXY*)	…	(*xxzY*)	…
		…	…	(*xzYY*)	(*xyYZ*)	…	(*yyzX*)	…
		…	…	**xyZZ**	**xzYZ**	…	**zzxY**	…
N_{ind}		15		36			30	
$N_{\neq 0}$		9		20			16	
N_{calc}		3		10			10	

they do not require application of a finite field along the periodic direction *x*.

Finite fields with different intensities (up to 0.02 a.u.) were applied along each non-periodic direction (*y*, *z*, and $y = z$). Field-dependent geometry optimizations followed by first-order perturbation theory (CP-SC1) calculations were used to generate the data for the left hand side of Eqs. (3), (8), and (10). In order to extract the nuclear relaxation (hyper)polarizabilities from Eqs. (4)–(6) and (11)–(13) an additional set of CP-SC1 calculations was performed at the field-free optimized geometry to obtain the pure static electronic (hyper)polarizabilities (and compare with coupled perturbed HF (CPHF) at the second-order perturbation level, CP-SC2).

III. COMPUTATIONAL DETAILS

Calculations were performed using a development version of the periodic *ab initio* CRYSTAL09 code,[9] that adopts a Gaussian-type basis set for constructing the Bloch functions. The latter are the variational basis for building the crystalline orbitals.

We have chosen to employ the HF level of theory in order to avoid the large overshoot in calculating the electronic (hyper)polarizability of PA (and other quasi-linear systems)[15–18,29–32] obtained with conventional DFT functionals, a phenomenon sometimes described as the *DFT catastrophe*.

Two computational parameters have been shown[32] to have a large influence on the calculated (hyper)polarizability tensors, namely, the shrinking factor *S* – defining the number of $\vec{k}$ points at which the self-consistent field (SCF) and CPHF equations are solved – and the pair of tolerances, collectively denoted as T_x, controlling the accuracy of the Hartree-Fock exchange series.[9,33] We set $T_x = T_4 = \frac{1}{2}T_5$ for the current calculations (see Ref. 9 for details). Optimal parameter values have been found in our previous work,[32] which shows that the smaller the band gap E_g the larger the values of *S* and T_x that need to be used. PA has a small energy gap due to π-electron conjugation ($1.6 \leq E_g \leq 1.8$ eV) (Ref. 34) which, we note in passing, is severely underestimated by pure DFT methods (for local-density approximation, LDA, and generalized-gradient approximation, GGA, $10^{-2} \leq E_g \leq 10^{-1}$ eV).[32] Although HF overestimates the band gap it yields much more reasonable (hyper)polarizabilities. Thanks to the large HF gap (about 7 eV),[32] it is sufficient to use $S = 30$ and $T_x = 100$. Convergence thresholds on the SCF energy and CP-SC (CP-SC1 and CP-SC2) steps were set to $T_E = 10$ and $T_{CP} = 4$, respectively.

A. Basis set

For molecules the calculation of optical properties requires the use of diffuse and polarization functions in conjunction with, say, an ordinary split-valence basis. However, in the case of periodic systems, the additional diffuse functions can lead to numerical problems due to linear dependence. Such functions are unnecessary for 3D systems where the ordinary split-valence basis functions of neighboring atoms compensate for their absence. This is not the situation for lower dimensionality systems (1D and 2D), e.g., PA, since the compensation is missing along non-periodic directions.

To tackle this problem, we added *ghost* atoms to a conventional 6-31G (all-electron) split-valence basis set in the following way. The *yz* space is tessellated by a number of equivalent *ghost* PA chains, surrounding the infinite periodic PA symmetrically. *Ghost* chains are arranged in parallel to the polymer plane (above/below, on the left/right) and in-phase with the original one (i.e., double bonds are lined up with double bonds and single bonds with single bonds). Distances with respect to an origin at the center of a C=C double bond are set to 3.5, 1.5, and 4.0 Å (and multiples) along directions *y*, *z*, and *yz*, respectively. Thus, a crown of *ghost* neighbors is defined around PA and the *ghost* atoms carry one valence *sp*

TABLE II. Static electronic (hyper)polarizability tensors, α^e and γ^e (in a.u.), of PA calculated by the CPHF method at different basis set levels. The 6-31G basis set has been used as a starting point and added with *ghost* functions progressively increasing in number and arranged according different (y, z) configurations with the origin at the mid-point of the carbon−carbon double bond and z perpendicular to the molecular plane. Configuration *A* includes 4 *ghost* molecules/cell at (0.0, ±1.5) and (± 3.5, 0.0) Å ; configuration *B* includes 10 *ghost* molecules/cell at (0.0, ±1.5), (± 3.5, 0.0), (0.0, ±3.0), and (± 2.0, ±3.5) Å ; configuration *C* includes 12 *ghost* molecules/cell at (0.0, ±1.5), (± 3.5, 0.0), (0.0, ±3.0), (± 2.0, ±3.5), and (± 7.0, 0.0) Å . Column |Δ| reports the percentage improvement between the numbers on the leftside column and those at the previous step. Values of the second hyperpolarizability along the longitudinal direction x in 10^6 a.u. Computational parameters: $T_E = 10$, $T_C = 10$, $T_x = 100$, $S = 30$.

			6-31G + *ghosts*					
		6-31G	*A*	|Δ| (%)	*B*	|Δ| (%)	*C*	|Δ| (%)
α	*xx*	165.29	170.7	3.3	171.5	0.5	171.5	0.0
	yy	18.46	19.81	7.3	19.89	0.4	19.89	0.0
	zz	5.996	13.07	118	13.45	2.9	13.45	0.0
γ	*xxxx*	6.193	6.040	2.5	5.968	1.2	5.964	0.1
	yyyy	−678.4	916.2	235	1250	36.4	1257	0.6
	zzzz	10.70	1486	1.38×10^4	2472	45.8	2472	0.0

shell (the same AO as the most diffuse one in the 6-31G basis set for C) attached to each atomic position. A similar method was adopted by Kirtman *et al.* in Ref. 35 for determining the (non)linear optical properties of LiF in quasi-linear and 2D structures.

Table II shows the effect of adding an increasing number of *ghost* AOs placed according to three different configurations (*A*, *B*, *C*, see the caption for details) around PA. The field-free equilibrium geometry has been used in each case. Neither α^e nor γ^e is substantially affected along the longitudinal direction x. The change in these properties due to the addition of the first set of *ghost* AOs arranged along the pure directions y and z (column *A*) does not reach 4% in either case. This is consistent with an extensive literature (e.g., Refs. 11, 14, and 32) which, since the late 80s,[11] has shown that the static longitudinal (hyper)polarizabilities of long chain polyenes are well-described using an ordinary split-valence 6-31G basis set.

On the contrary, the effect of the ghost functions on the non-periodic components is very large, particularly for γ^e. Addition of *ghost* AOs in configuration *A*, causes γ^e_{yyyy} to change by 235% – including a change of sign – and increases γ^e_{zzzz} by a factor of nearly 150, while the non-periodic diagonal components of α^e are altered by up to 118% (*cf.*, α^e_{zz}).

Further addition of *ghost* functions along directions z and yz (column *B*) does not have a significant effect on the polarizabilities α^e_{yy} or α^e_{zz}. However, γ^e_{zzzz} increases by about 50% while γ^e_{yyyy} grows simultaneously by 36%. Nonetheless, the further addition of another set of *ghost* chains along y (column *C*) has a negligible (less than 1%) effect on every property. Thus, configuration *B* was adopted for all calculations in the present work.

One may wonder about the accuracy of the present scheme. As a check we considered the shortest oligomer of PA, i.e., ethylene, C_2H_4, and performed CPHF calculations using different basis sets specifically optimized for molecular calculations of the polarizability[36,37] and hyperpolarizabilities.[38,39] Even the shortest oligomer provides a good test because the (hyper)polarizabilities in the non-periodic directions converge rapidly with chain length. Table III compares the performance of our [6-31G+*B*] combination (as defined in Table II) with that of the above mentioned molecular basis sets. Only the non-periodic directions are considered since we have already established that the longitudinal properties of the infinite periodic chain are hardly affected by adding the ghost functions. For α_{yy} and α_{zz} there is excellent agreement between the [6-31G+*B*] basis set and the better molecular basis sets. More critical is the assessment of γ. In that event we find that the [6-31G+*B*] values agree reasonably well with those determined using the Z3PolX basis set,[38,39] which was designed specifically for the treatment of hyperpolarizabilities. Much smaller values, especially for γ_{zzzz}, were obtained with the so-called def2 basis sets,[36] but the latter were designed for polarizability, rather than hyperpolarizability, calculations. Thus, we conclude that the diagonal components of γ in the transverse and perpendicular directions provide a sensitive and successful test of the [6-31G+*B*] basis set.

TABLE III. Static electronic CPHF (hyper)polarizabilities – α^e and γ^e (in a.u.) – of ethylene calculated by using different molecular basis sets, specifically optimized for the estimation of optical properties.[36–39] Comparison with the split-valence 6-31G basis set and the [6-31G+*B*] set (used for periodic 1D calculations) is made. Computational parameters as in Table II.

	α^e		γ^e	
	yy	*zz*	*yyyy*	*zzzz*
def2-SVPD[36]	23.27	20.53	1659	1122
def2-TZVPD[36]	23.93	22.02	2269	2575
def2-TZVPPD[36]	23.94	21.97	2251	2736
Sadlej-pVTZ[37]	23.91	22.34	2820	1.175×10^4
Z3PolX[38,39]	24.20	21.91	2257	7492
6-31G	19.19	7.149	366.0	16.70
[6-31G+*B*]	23.68	21.97	2826	8965

The addition of ghost functions to the 6-31G basis set does not come without substantial cost. Using configuration *B* of Table II increases the number of AOs per unit cell from 22 to 182. In comparison to 6-31G (running on 8 intel64 cores and under the same computational conditions): (1) a very well converged single point [6-31G+*B*] calculation takes about 1 h, or about 600 times longer; (2) each geometry optimization point (i.e., SCF *plus* Hessian updating) takes about 7 h *vs.* 7 s for 6-31G; and (3) a CPHF cycle takes about 3 h *vs.* 12 s for 6-31G. We believe that a more sophisticated choice of distributed Gaussian functions can be made to achieve a major savings of computer time, but leave that to future work.

IV. RESULTS AND DISCUSSION

A. Field free calculations and numerical accuracy

The field-free equilibrium geometry (R_0) of PA has been used to obtain the pure electronic tensors α^e and γ^e by the

TABLE IV. Static electronic polarizability α^e (in a.u.) of PA calculated by the CPHF and FF methods at the field-free equilibrium geometry. Calculations have been performed using the [6-31G+B] basis set. Equation (2) was employed to fit the dipole moment *versus* the finite field to provide numerical estimates of α^e. Computational parameters as in Table II.

	CPHF	Fitted values
xx	171.5	...
xy	17.48	...
yy	19.89	19.89
zz	13.45	13.45

analytical CPHF method[40–43] (β^e is null by symmetry). For comparison, α^e and γ^e can also be found by expanding μ^e_t, α^e_{tu}, and β^e_{tuv} as functions of an applied (transverse and/or perpendicular) finite field, according to Eqs. (2), (7), and (9). The FF expansions yield the static α^e_{yy} and α^e_{zz} (Table IV), as well as eight out of nine independent, non-zero components of the static γ^e tensor (Table V); since the FF scheme along periodic directions is not yet implemented in CRYSTAL, γ^e_{xxxx} is not available for this comparison. In fact, duplicate estimates for the γ^e components were obtained from the cubic, quadratic, and linear coefficients in the expansion of $\mu^e(R_0; F)$, $\alpha^e(R_0; F)$, and $\beta^e(R_0; F)$ *vs* F, respectively. As expected, the agreement with the analytical CPHF results is better when fitting lower order finite field coefficients. In the worst case the difference with CPHF does not exceed 5% and in all other instances it is less than 2%. The uncertainty on numerical fitting parameters is very small as well, i.e., always within 2%. Moreover, the permutation symmetry is satisfactorily maintained, e.g., γ^e_{yyzz} can be determined either by fitting $\alpha^e_{yy}(R_0; F)$ *vs* F_z, or $\alpha^e_{zz}(R_0; F)$ *vs* F_y, or $\alpha^e_{yz}(R_0; F)$ *vs* $F_y = F_z$; the corresponding γ^e coefficients in the three cases differ by no more than 2.5%. Tables IV and V document the high accuracy achieved in all instances. This suggests that the numerical procedure adopted for determining the vibrational contribution to α and γ will be reliable as well.

TABLE V. Static electronic second hyperpolarizability γ^e (in a.u.) of PA calculated at the field-free equilibrium geometry by the CPHF and FF methods. Columns (a), (b), and (c) report numerical estimates obtained by fitting the dipole moment, polarizability, and first hyperpolarizability (Eqs. (2), (7) and (9)), respectively, *versus* a finite field. The four classes of components (i. - iv.) are defined in Section II C and Table I. Basis set and computational details as in Table IV.

			Fitted values		
		CPHF	(a)	(b)	(c)
(i)	$yyyy$	1250	1300	1289	1246
	$zzzz$	2472	2504	2498	2473
(ii)	$xxxy$	1.344×10^5	...	...	1.348×10^5
	$xyyy$	−3572	...	−3541	−3570
(iii)	$xxyy$	-1.344×10^4	...	-1.343×10^4	-1.345×10^4
	$xxzz$	5706	...	5711	5692
	$yyzz$	608.1	638.0	613.8	608.0
(iv)	$xyzz$	219.9	...	221.1	218.9

B. Effect of applied electric field on energy, band gap, and geometry

The relaxation energy as a function of the field intensity (field along y or z) is relatively small (less than 1.5 mHa per C_2H_2 unit for a field up to 0.02 a.u.). Likewise, the structural deformation is small, for example, a mixed field $F_y = F_z = 0.015$ a.u. induces an extension of the C−C double bond length by about 1.5×10^{-3} Å and a reduction in the bond length alternation (BLA) of less than 2%. Perpendicular fields, of course, break planarity; the hydrogen atoms are displaced by 0.017 Å out-of-plane under a field of magnitude 0.02 a.u. while the carbon atoms are displaced a like amount in the opposite direction. Finally, a significant variation occurs on the band gap E_g, which is reduced by about 23% for a field of up to 0.02 a.u. along z.

C. Nuclear relaxation contributions to the polarizability and the second hyperpolarizability

The nuclear relaxation (ionic) contributions to the diagonal transverse and perpendicular static polarizabilities, $\alpha^{nr}_{YY} = 0.04$ and $\alpha^{nr}_{ZZ} = 0.96$ a.u., are both small compared to the corresponding electronic contributions (Table VI). Numerical values from fitting Eq. (3) and analytical values from Eq. (1) (obtained using the full set of frequencies and Born charges in the Berry phase approach) compare very well (to the number of significant figures reported). The numerical values are given by the difference in the intercepts for the two curves in the top row of Figure 1, i.e., $\alpha^{nr}_{YY} = 0.03$ and $\alpha^{nr}_{ZZ} = 0.97$ a.u., which are plots of μ/F *vs* F (y and z directions) with and without nuclear relaxation. Clearly, the nuclear relaxation contribution in the perpendicular direction is more important than in the transverse direction: $a^{\mu}_{zz} = 14.42$ a.u. exceeds $\alpha^e_{zz} = 13.45$ a.u. by about 7% (the corresponding difference in the y direction is less than 0.2%).

Table VI summarizes results obtained for all non-vanishing components of α^{nr} (the xx and xy components were obtained by the Berry phase approach) as well as α^e. We note that the diagonal nuclear relaxation contribution along the periodic direction turns out to be very small (0.18 a.u.) compared to the value extrapolated from finite chains by Champagne *et al.*,[13] i.e., 14.35 ± 0.90 a.u. (which, itself, is only about 10% of the corresponding electronic polarizability). The large difference between the oligomer and periodic polymer values is a consequence of the fact that the low frequency transverse collective modes of oligomers, which give rise to a *longitudinal* dipole moment,[14] are not included in the periodic polymer calculations. In the oligomer both the frequency ν_j and the longitudinal Born charge $\overline{Z}_x$ decrease with increasing chain length, but in such a way that a non-zero value is obtained[14] for the square of the ratio (see Eq. (1)) in the infinite chain limit. The treatment of this piezoelectric acoustic vibrational contribution in 1D periodic calculations will be addressed in future work.

Table VII summarizes our results for the contribution to the second hyperpolarizability due to nuclear motions. As expected, the vibrational components become larger (in

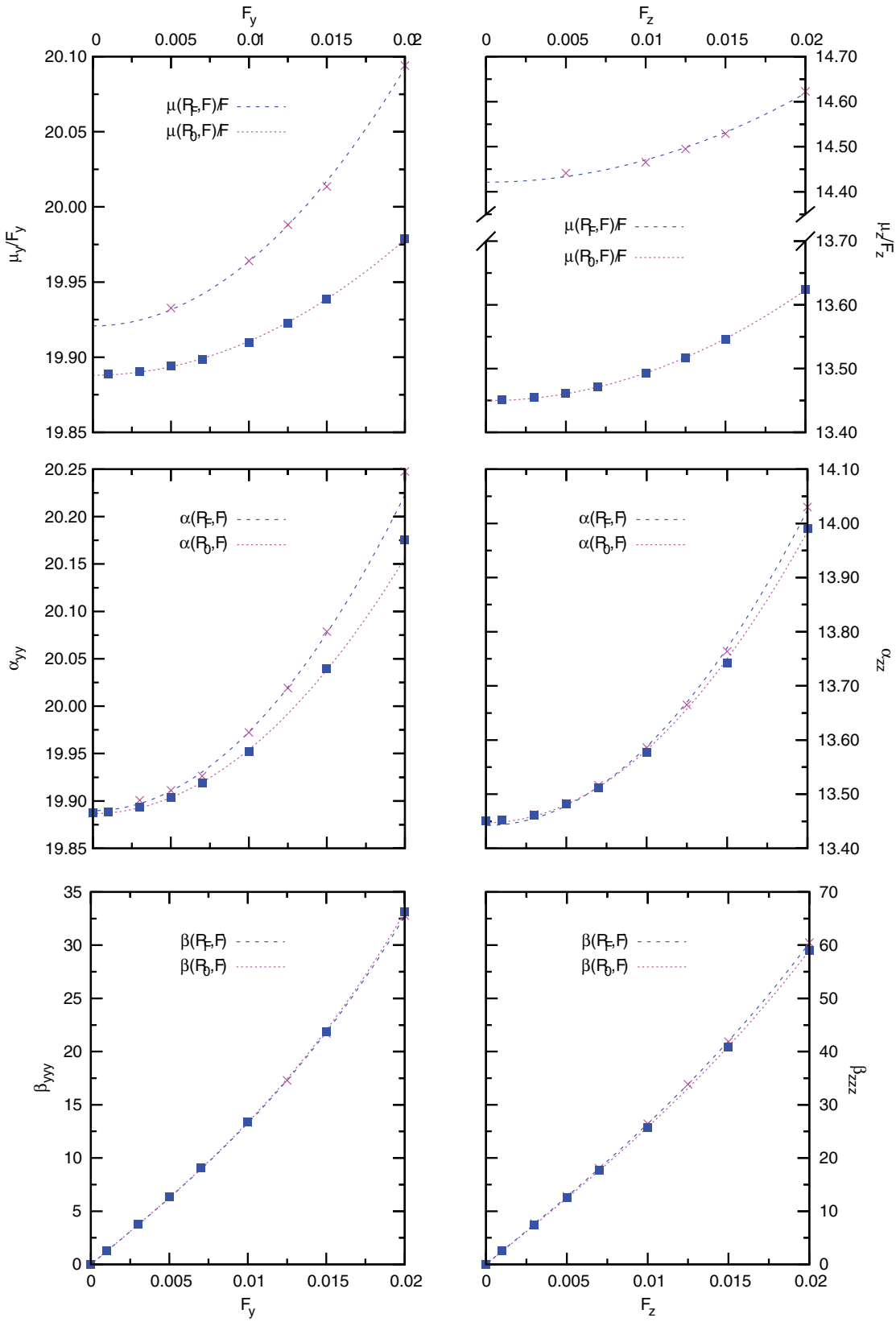

FIG. 1. μ/F, α and β of PA *vs* a finite field F (in a.u.) applied along the non-periodic transverse (y; left) and perpendicular (z; right) directions. Calculations at the field-free optimized structure provide the electronic contributions to α and γ (α^e and γ^e, respectively) as coefficients in the expansions (2), (7), and (9). Structural relaxation in the presence of the field (R_F) provides, in addition, the vibrational contributions according to Eqs. (3), (8), and (10). Calculations performed at the HF/[6-31G+B] level. Computational parameters: $T_E = 10$, $T_C = 10$, $T_x = 100$, $S = 30$.

TABLE VI. Static vibrational (nuclear relaxation), α^{nr}, and electronic, α^{e} contributions to the independent, non-vanishing polarizability components of PA. Analytical values obtained using the Berry phase approach (α^{nr}) and the CPHF method (α^{e}) are reported. Basis set and computational details as in Table IV.

	α^{nr}	α^{e}
xx	0.182	171.5
xy	−0.087	17.48
yy	0.042	19.89
zz	0.959	13.45

absolute value) as the number of static field indices increases. The γ_2^{nr} components are about 5 (*yyzz*) to 167 (*xxyy*) times larger than the corresponding γ_1^{nr} components. The γ_4^{nr} hyperpolarizability components range up to about 3.3 times larger than the corresponding γ_2^{nr} values, although they may be smaller in some cases as well.

In general, the various components of γ_1^{nr} are nearly two orders of magnitude smaller than the corresponding static electronic term reported in Table V. Vibrational γ_2^{nr} values are comparable in magnitude to, or a bit larger than, the static electronic (γ^{e}) contributions for those components involving one or more *x* indices. In almost all other cases, the ratio γ_2^{nr}/γ^{e} is less than 0.5, whereas γ_4^{nr} tends to be comparable to γ^{e} also for transverse and perpendicular fields.

D. Experimental implications

We are not aware of any experimental data that bears on the major issue of this paper, namely the relative magnitude of vibrational *vs.* electronic contributions to static and dynamic third-order susceptibilities of PA. There are measurements of third harmonic generation (THG) on non-oriented and oriented thin films,[44–46] but in that case the vibrational contribution is predicted to be very small; in fact, it is zero in the IOFA. A comparison with CPHF/6-31G calculations for the pure electronic THG has been made[47] and a number of reasons advanced as to why the calculated result is too small. These reasons include, among others, the theoretical treatment being based on an isolated chain model and restricted to the non-resonant regime. Moreover, there are the limitations of the CPHF method which omits the effect of correlation on the computed (hyper)polarizabilities in addition to yielding an overly long BLA and an excessive band gap, as emphasized in this paper and previously.[32] All of the aforementioned aspects remain pertinent for the present calculations. The purpose of our work is not to give a faithful reproduction of experimental data, but rather an estimate of the ratio between vibrational and electronic contributions to the properties considered here. In this connection, it should be noted that typical measurements only provide the sum of electronic and vibrational contributions. From the ratio, however, one can separate these two terms and, thereby, provide a further analysis of the experiments.

V. CONCLUSIONS

The vibrational contribution to the linear polarizability and (second)hyperpolarizability tensors of polyacetylene was evaluated by means of the FF-NR scheme at the HF/[6-31G+*B*] level. Here, the notation [6-31G+*B*] refers to a basis set containing *ghost* AOs that was specially developed in order to provide accurate electronic hyperpolarizabilities, especially in the direction perpendicular to the molecular plane. The FF-NR scheme yields values for dynamic (infinite optical frequency approximation) as well as static processes. Our calculations were carried out using an extension of the original FF-NR method to periodic systems implemented in the CRYSTAL code. Approximately half of the independent, non-zero components for each process were obtained. The remainder require a geometry optimization in the presence of a finite

TABLE VII. FF-NR static and dynamic vibrational (nuclear relaxation) contributions to the second hyperpolarizability γ (in a.u.) of PA obtained by fitting (a) the dipole moment, (b) the polarizability and (c) the first hyperpolarizability *versus* the finite field according to Eqs. (3), (8) and (9). The uncertainty in the fitted parameters is, generally, within 5%; dashes indicate components that are currently inaccessible. For basis set, computational, and other details see Table IV.

		Fitted values					
		(a)		(b)		(c)	
Class		g^{μ}	γ_4^{nr}	g^{α}	γ_2^{nr}	g^{β}	γ_1^{nr}
(i)	*yyyy*	2419	1169	1672	422	1223	−27
	zzzz	2843	371	2780	308	2514	42
(ii)	*xxxy*	…	…	…	…	1.373×10^5	2900
	xyyy	…	…	1675	5247	−3614	−42
(iii)	*xxyy*	…	…	9877	2.332×10^4	-1.358×10^4	−140
	xxzz	…	…	1.158×10^4	5874	5766	60
	yyzz	1541	933	861.9	253.8	658.1	50
	yzyz	1541	933	1855	1247	658.1	50
	zzyy	1541	933	672.4	64.3	602.6	−5.5
(iv)	*xyzz*	…	…	879.4	659.5	250.2	30.3
	xzyz	…	…	2740	2520	250.2	30.3
	xzzy	…	…	2740	2520	220.0	0.1

longitudinal (periodic direction) field, which involves methodology that is in the development stage, but not currently available. Nonetheless, depending upon the process, many components involving the longitudinal direction could be accessed.

The correctness and numerical accuracy of our implementation was checked by comparing numerical finite field results with analytical CPHF calculations for static electronic properties. A similar comparison between vibrational contributions to the linear polarizability, obtained either by the FF-NR method or by the analytical Berry phase approach, also indicated the reliability of our numerical results. By far the largest source of uncertainty in the values reported lies in the HF/[6-31G+B] method of calculation. A comparison for ethylene shows good agreement with the Z3PolX basis set of Refs. 38 and 39. However, the Hartree-Fock Hamiltonian, chosen in order to avoid the *DFT catastrophe*, does not account for correlation effects that are known to be important in molecular calculations. In this regard, a reliable DFT method that would reduce the uncertainty is highly desirable.

Although vibrations play a minor role in determining the linear polarizability, they are very important as far as the second hyperpolarizability is concerned. Their contribution, as compared to the corresponding static electronic component, is dictated primarily by the number of static fields used to characterize the nonlinear process. The ratio γ^{nr}/γ^{e}, which is maximum for γ_4^{nr} (all static fields), decreases for two static fields (γ_2^{nr}; DC-Kerr effect), and more so for one field (γ_1^{nr}; DC-second harmonic generation). The ratio is on the order of unity for the DC-Kerr effect and static γ, whereas the ionic contibution to the DC-second harmonic generation is not as important.

As noted above we are pursuing the treatment of finite fields in the periodic direction. Our efforts are based on the phase-smoothing procedure used in the so-called vector potential approach described in Ref. 26 (and references therein). This will set the stage for piezoelectric applications as well as generalization to 2D and 3D periodic systems. In addition, efforts along two lines are planned to reduce computation times: (1) introduction of so-called field-induced coordinates, which are known to be effective in molecular calculations;[48,49] and (2) development of more compact basis sets for non-periodic directions.

[1] B. Kirtman and D. Bishop, Chem. Phys. Lett. **175**, 601 (1990).
[2] D. M. Bishop, M. Hasan, and B. Kirtman, J. Chem. Phys. **103**, 4157 (1995).
[3] B. Kirtman, J. M. Luis, and D. M. Bishop, J. Chem. Phys. **108**, 10008 (1998).
[4] B. Kirtman and J. M. Luis, J. Chem. Phys. **128**, 114101 (2008).
[5] M. B. Hansen, O. Christiansen, and C. Hattig, J. Chem. Phys. **131**, 154101 (2009).
[6] B. Kirtman and J. Luis, Int. J. Quantum Chem. **111**, 839 (2011).
[7] M. Ferrabone, B. Kirtman, R. Orlando, M. Rérat, and R. Dovesi, Phys. Rev. B **83**, 235421 (2011).
[8] C. Pisani, R. Dovesi, and C. Roetti, *Hartree-Fock Ab-Initio Treatment of Crystalline Systems* (Springer-Verlag, 1988), p. 96.
[9] R. Dovesi, V. R. Saunders, C. Roetti, R. Orlando, C. M. Zicovich Wilson, F. Pascale, K. Doll, N. M. Harrison, B. Civalleri, I. J. Bush, Ph. D'Arco, and M. Llunell, *CRYSTAL09 User's Manual* (Università di Torino, Torino, 2009).
[10] S. Suhai, J. Chem. Phys. **73**, 3843 (1980).
[11] G. Hurst, M. Dupuis, and E. Clementi, J. Chem. Phys. **89**, 385 (1988).
[12] M. Ferrabone, B. Kirtman, V. Lacivita, M. Rérat, R. Orlando, and R. Dovesi, Int. J. Quantum Chem. **112**, 2160 (2011).
[13] B. Champagne, E. A. Perpéte, and J.-M. André, J. Chem. Phys. **101**, 10796 (1994).
[14] B. Kirtman, B. Champagne, and J. André, J. Chem. Phys. **104**, 4125 (1996).
[15] B. Champagne, E. A. Perpéte, S. J. A. van Gisbergen, E. J. Baerends, J. Snijders, C. Soubra Ghaoui, K. A. Robins, and B. Kirtman, J. Chem. Phys. **109**, 10489 (1998).
[16] B. Champagne, E. A. Perpéte, S. J. A. van Gisbergen, E. J. Baerends, J. Snijders, C. Soubra Ghaoui, K. A. Robins, and B. Kirtman, J. Chem. Phys. **110**, 11664 (1999).
[17] S. van Gisbergen, P. Schipper, O. Gritsenko, E. Baerends, J. Snijders, B. Champagne, and B. Kirtman, Phys. Rev. Lett. **83**, 694 (1999).
[18] S. Kummel, L. Kronik, and J. Perdew, Phys. Rev. Lett. **93**, 213002 (2004).
[19] H. Sekino, Y. Maeda, M. Kamiya, and K. Hirao, J. Chem. Phys. **126**, 014107 (2007).
[20] B. Kirtman, S. Bonness, A. Ramirez-Solis, B. Champagne, H. Matsumoto, and H. Sekino, J. Chem. Phys. **128**, 114108 (2008).
[21] D. Jacquemin, E. Perpéte, I. Ciofini, and C. Adamo, J. Comput. Chem. **29**, 921 (2008).
[22] P. Limacher, K. Mikkelsen, and H. Lüthi, J. Chem. Phys. **130**, 194114 (2009).
[23] R. Resta, Rev. Mod. Phys. **66**, 899 (1994).
[24] S. Dall'Olio, R. Dovesi, and R. Resta, Phys. Rev. B **56**, 10105 (1997).
[25] C. Zicovich-Wilson, R. Dovesi, and V. Saunders, J. Chem. Phys. **115**, 9708 (2001).
[26] M. Springborg and B. Kirtman, Theor. Chem. Acc. **130**, 687 (2011).
[27] M. Torrent-Sucarrat, M. Solá, M. Duran, J. M. Luis, and B. Kirtman, J. Chem. Phys. **120**, 6346 (2004).
[28] D. Shelton, J. Chem. Phys. **84**, 404 (1986).
[29] B. Champagne, E. Perpéte, D. Jacquemin, S. van Gisbergen, E. Baerends, C. Soubra Ghaoui, K. Robins, and B. Kirtman, J. Phys. Chem. A **104**, 4755 (2000).
[30] M. van Faassen, P. de Boeij, R. van Leeuwen, J. Berger, and J. Snijders, J. Chem. Phys. **118**, 1044 (2003).
[31] M. van Faassen, P. de Boeij, R. van Leeuwen, J. Berger, and J. Snijders, Phys. Rev. Lett. **88**, 186401 (2002).
[32] V. Lacivita, M. Rèrat, R. Orlando, M. Ferrero, and R. Dovesi, J. Chem. Phys. **136**, 114101 (2012).
[33] M. Causá, R. Dovesi, R. Orlando, C. Pisani, and V. R. Saunders, J. Chem. Phys. **92**, 909 (1988).
[34] C. Fincher, C. Chen, A. Heeger, A. MacDiarmid, and J. Hastings, Phys. Rev. Lett. **48**, 100 (1982).
[35] B. Kirtman, V. Lacivita, R. Dovesi, and H. Reis, J. Chem. Phys. **135**, 154101 (2011).
[36] D. Rappoport and F. Furche, J. Chem. Phys. **133**, 134105 (2010).
[37] A. Sadlej, Theor. Chem. Acc. **81**, 339 (1992).
[38] Z. Benkova, A. Sadlej, R. Oakes, and S. Bell, J. Comput. Chem. **26**, 145 (2005).
[39] Z. Benkova, A. Sadlej, R. Oakes, and S. Bell, Theor. Chem. Acc. **113**, 238 (2005).
[40] M. Ferrero, M. Rérat, R. Orlando, and R. Dovesi, J. Comput. Chem. **29**, 1450 (2008).
[41] M. Ferrero, M. Rérat, R. Orlando, R. Dovesi, and I. Bush, J. Phys.: Conf. Ser. **117**, 12016 (2008).
[42] M. Ferrero, M. Rérat, B. Kirtman, and R. Dovesi, J. Chem. Phys. **129**, 244110 (2008).
[43] R. Orlando, V. Lacivita, R. Bast, and K. Ruud, J. Chem. Phys. **132**, 244106 (2010).
[44] M. Drury, Solid State Commun. **68**, 417 (1988).
[45] A. Heeger, D. Moses, and M. Sinclair, Synth. Met. **17**, 343 (1987).
[46] F. Krausz, E. Wintner, and G. Leising, Phys. Rev. B **39**, 3701 (1989).
[47] F. Gu, D. Bishop, and B. Kirtman, J. Chem. Phys. **115**, 10548 (2001).
[48] J. Luis, M. Duran, B. Champagne, and B. Kirtman, J. Chem. Phys. **113**, 5203 (2000).
[49] J. Luis, M. Duran, and B. Kirtman, J. Chem. Phys. **115**, 4473 (2001).